Thermo-optic hysteresis induced by a high-quality defect mode in a two-dimensional photonic crystal

G. V. Shadrina [1], E. N. Bulgakov [1,2], D. N. Maksimov [1,2,3] and V. S. Gerasimov [1]

[1]*Institute of Computational Modelling SB RAS, Krasnoyarsk 660036, Russia*
[2]*Kirensky Institute of Physics, Federal Research Center KSC SB RAS, Krasnoyarsk 660036, Russia*
[3]*IRC SQC, Siberian Federal University, Krasnoyarsk 660041, Russia*

We consider thermo-optic bistability induced by a high-quality defect mode in the square array of dielectric rods. It is demonstrated that the scattering problem with an account of the variation of the dielectric constant by heating can be solved with the T-matrix method by introducing an explicit dependence of the permittivity of the defect rod on temperature. We found that the bistability occurs at low intensities of the incident wave $\approx 0.01 \text{mW}/\mu\text{m}^2$ in a square array of 7×7 silicon rods with a defect rod in the middle.

I. INTRODUCTION

Thermophotonics is an important branch of nano-optics dealing with various temperature effects induced by heating the system by the absorbed light [1–6]. One such temperature effect emerging in thermophotonic systems is nonlinearity due to thermorefractive phenomena [7–12]. Recently, we have seen a surge of interest in all-dielectric nanophotonics [13,14]. In comparison with plasmonic systems the all-dielectic structure exhibits low material absorption which seemingly prohibits effective light-to-heat conversion. This, however, can be circumvented by engineering the effect of critical coupling [15–17] which leads to highly efficient light absorbers [18–22] to be used for enhanced light-to-heat conversion. Lately, it has been pointed out that thermo-optical effects can be dominant nonlinear effects in resonant nanophotonic structures subject to high-intensity incident fields due to heating by absorbed radiation [23].

The key element for strong thermo-optical effects in all-dielectric systems is setting up a nanophotonic structure supporting high-quality resonances which have become an important tool for enhanced light-matter interactions [13,14,22]. One of the possible approaches is to employ optical bound states in the continuum (BICs) [24–26], i.e., nonradiating modes embedded in the continuous spectrum of scattering solutions above the line of light. In the presence of material absorption the BICs still have a finite lifetime but nonetheless remain localized and decoupled from the outgoing channels [27]. Once the system's symmetry is broken, either by design [28] or by the incident light [29], the BICs are transformed to high-quality resonances known as quasi-BICs.

Another route is the application of isolated dielectric resonators, which have been shown to support high-quality resonance similar to quasi-BICs [30]. Thermo-optical effects have been widely studied in various single resonator setups, including plasmonic [1,31,32], all-dielectric [33–36], and graphene-based [37] structures. In this paper we shall employ the high-quality resonant defect mode [38,39] supported by a two-dimensional (2D) all-dielectric photonic crystal made of SiO$_2$ subwavelength rods of circular cross section. We shall demonstrate that such a platform can be used as an efficient alternative tool observing optical bistability with an intensity threshold lower than that reported for a single rod (cylinder).

II. SCATTERING BY THE ARRAY OF RODS

We consider the system shown in Fig. 1(a). The system is a rectangular array of dielectric rods made of Si with radius R_0 packed in a square $N \times N$ lattice with period a. The central rod, highlighted in blue in Fig. 1(a), has a different radius R_d. This rod plays the role of a defect in the photonic-crystalline lattice. In what follows, we consider transverse-magnetic (TM) waves in 2D in which case the electric field is aligned with the z axis and the problem is reduced to finding the z component E_z. In the case of infinite N the system is a 2D photonic crystal that supports a microcavity mode localized at the defect rod. We take $R_0 = 0.18a$, $R_d = 0.08a$. If the array is finite, the quality factor is limited by tunneling across the Bragg mirrors. For an array of $N \times N = 49$ we obtained $Q \approx 4 \times 10^3$ [40]. The band structure of an infinite crystal without defects is shown in Fig. 1(b). The vacuum wave number of the defect mode $ak_0 = 0.35217$ is shown by a dashed line in the middle of the band gap. The mode profile is shown in Fig. 1(c).

Before analyzing the thermo-optic effect we would like to outline the method of solving the scattering problem. The method applied in this work is known as the T-matrix method and is thoroughly described in Ref. [41]. Here, we restrict ourselves to a brief overview necessary for further consideration of the thermo-optic effects. First, the field inside the j_{th} rod is written as

$$E_z = \sum_{m=-\infty}^{\infty} c_{j,m} J_m(\sqrt{\epsilon_j} k_0 r_j) e^{im\phi_j}, \quad (1)$$

where J_m is the Bessel function of the first kind, ϵ_j is the j_{th} rod permittivity, k_0 is the vacuum wave number of the incident wave, r_j, ϕ_j are the local cylindrical coordinates with
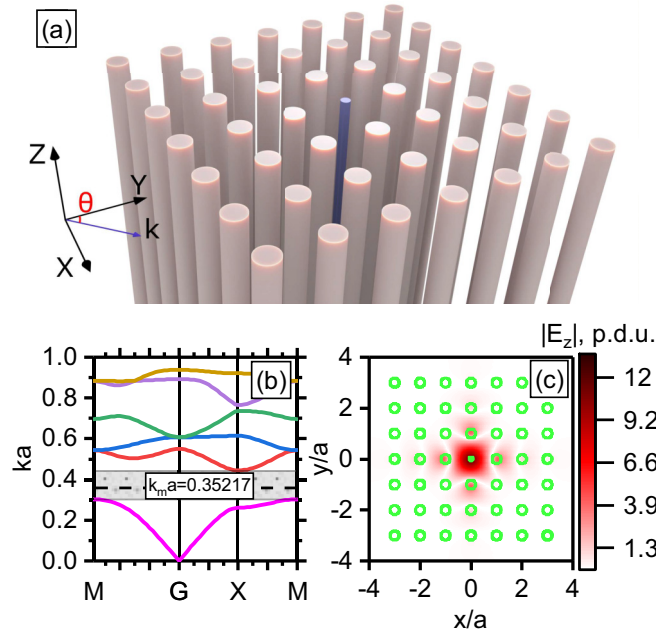
FIG. 1. Defect mode in a rectangular array of dielectric rods. (a) Setup of the array of Si dielectric rods. (b) The band structure of the rectangular array of rods with the vacuum wave number of the defect mode shown in the middle of the band gap by a dashed line. (c) The defect mode profile.

the origin in the centerline of the jth rod, and, finally, $c_{j,m}$ are unknown expansion coefficients. At the same time outside the rods we have

$$E_z = \sum_{m=-\infty}^{\infty} \left[a_{j,m} J(k_0 r_j) + b_{j,m} H_m^{(1)}(k_0 r_j) \right] e^{im\phi_j}, \quad (2)$$

where $H_m^{(1)}$ is the outgoing Hankel function, $a_{j,m}$ are the incident amplitudes, and $b_{j,m}$ are the reflected amplitudes. The incident amplitudes are further decomposed as follows,

$$a_{j,m} = a_{j,m}^{(\text{in})} + a_{j,m}^{(\text{rods})}, \quad (3)$$

where $a_{j,m}^{(\text{in})}$ describes the incident wave, and $a_{j,m}^{(\text{rods})}$ is the contribution from scattering by the other than the jth rod. In the case of the plane wave we have

$$a_{j,m}^{(\text{in})} = (-1)^m e^{ik_0 R_j \sin(\theta_{\text{in}} - \theta_j) - im\theta_{\text{in}}}, \quad (4)$$

where R_j and θ_j are the coordinates of the jth rod in the global cylindrical coordinate system. The amplitudes $a_{j,m}^{(\text{rods})}$ can be related to the outgoing amplitudes $b_{j,m}$ via Graf's addition theorem which states that

$$a_{j,m}^{(\text{rods})} = \sum_q \sum_{\ell \neq j} b_{\ell,q} e^{i(m-q)\theta_{j,\ell}} H_{m-q}^{(1)}(k_0 r_{j,\ell}), \quad (5)$$

where $r_{j,\ell}$ is the distance between the jth and ℓth rods while $\theta_{j,\ell} = \theta_j - \theta_\ell$ is the difference of their azimuthal coordinates in the global coordinate system (see Fig. 1). As a result one obtains the following system of equations,

$$\mathbf{a}_j = \mathbf{a}_j^{(\text{in})} + \sum_{\ell \neq j} \widehat{T}_{j,\ell} \mathbf{b}_\ell, \quad (6)$$

where $\mathbf{a}_j^{(\text{in})}$ and $\mathbf{b}_j$ are the vectors assembled from amplitudes $a_{j,m}^{(\text{in})}$ and $b_{j,m}$, correspondingly, while the elements of $\widehat{T}_{j,\ell}$ are defined as follows,

$$\{\widehat{T}_{j,\ell}\}_{m,q} = e^{i(q-m)\theta_{j,\ell}} H_{m-q}^{(1)}(k_0 r_{j,\ell}). \quad (7)$$

Equation (6) can be rewritten as a closed set of equations by using diagonal matrices $\hat{t}_j$ which solve the scattering problem for individual rods,

$$\mathbf{b}_j = \hat{t}_j \mathbf{a}_j. \quad (8)$$

The elements of the matrices $\hat{t}_j$ have the following form,

$$\{\hat{t}_j\}_{m,m} = -\frac{\sqrt{\epsilon_j} J_m(k_0 R_j) J_m'(k_0 \sqrt{\epsilon_j} R_j) - k_0 J_m(k_0 \sqrt{\epsilon_j} R_j) J_m'(k_0 R_j)}{\sqrt{\epsilon_j} H_m^{(1)}(k_0 R_j) J_m'(k_0 \sqrt{\epsilon_j} R_j) - k_0 J_m(k_0 \sqrt{\epsilon_j} R_j) H_m^{(1)'}(k_0 R_j)}. \quad (9)$$

As the final result we have

$$\mathbf{b}_j - \sum_{\ell \neq j} \hat{t}_j \widehat{T}_{j,\ell} \mathbf{b}_\ell = \hat{t}_j \mathbf{a}_j^{(\text{in})}. \quad (10)$$

III. HEAT TRANSFER

Before proceeding to the thermo-optical effect, we have to address the heat transfer in the system under scrutiny. In our analyses we assume that the power of the incident light is only absorbed in the defect rod since we are only interested in the resonant effects due to excitation of the mode depicted in Fig. 1(c). Here, we have to solve the heat equation

$$-\nabla \cdot [\varkappa(\mathbf{r})\nabla\Theta(\mathbf{r})] = \frac{1}{S}Pf(\mathbf{r}), \quad (11)$$

where $\varkappa(\mathbf{r})$ is the heat transfer coefficient, P is the absorbed power, $f(\mathbf{r})$ is the function equal to unity within the defect rod being zero everywhere else, and S is the area of the cross section of the defect rod. We apply the Dirichlet boundary conditions outside of the array with room temperature $\Theta_r = 300$ K. The heat transfer coefficient $\varkappa(\mathbf{r})$ is coordinate dependent. We use $\varkappa_S = 156$ W/(m K) within the silicon rods and $\varkappa_0 = 0.02$ W/(m K) in air. For numerical simulations we shall use the nondimensionalized form of Eq. (11),

$$\bar{\nabla} \cdot \left[\frac{\varkappa(\mathbf{r})}{\varkappa_0} \bar{\nabla}\Theta(\bar{\mathbf{r}}) \right] = \frac{a^2 P}{\varkappa_0 S} f(\bar{\mathbf{r}}), \quad (12)$$

where $\bar{\nabla}$ uses differentiation with respect to the new variable,

$$\bar{\mathbf{r}} = \frac{1}{a}\mathbf{r}. \quad (13)$$

Let $\bar{\Theta}(\bar{\mathbf{r}})$ be the solution of

$$\bar{\nabla} \cdot \left[\frac{\varkappa(\mathbf{r})}{\varkappa_0} \bar{\nabla} \bar{\Theta}(\bar{\mathbf{r}}) \right] = f(\bar{\mathbf{r}}). \quad (14)$$

Assuming that the defect rod is uniformly heated since the Biot number is small [17] we can take $f(\bar{\mathbf{r}})$ equal to identity within the rod and zero everywhere else. After finding $f(\bar{\mathbf{r}})$ we can write for the temperature increment within the defect rod

$$\Delta\Theta = \frac{a^2 \bar{\Theta}_0 P}{\varkappa_0 S}, \quad (15)$$

where $\bar{\Theta}_0$ is the value of $\bar{\Theta}(\bar{\mathbf{r}})$ in the center of the defect rod. Then the effective heat transfer coefficient at the boundary of the defect rod is given by

$$\bar{\varkappa} = \frac{a^2}{\varkappa_0 \pi R_d^2} \bar{\Theta}_0. \quad (16)$$

IV. THERMO-OPTICAL EFFECTS

The thermo-optical effect under consideration is due to the change of the dielectric permittivity

$$\epsilon = \epsilon' + i\epsilon'' \quad (17)$$

by heating. We assume that the refractive index is dependent on the temperature

$$n = n_0 + n_1 \Delta\Theta, \quad (18)$$

where $n_1 = 2 \times 10^{-4} \frac{1}{\text{K}}$. Thus, we have

$$\epsilon' = \epsilon_0 + 2\sqrt{\epsilon_0} n_1 \Delta\Theta. \quad (19)$$

The heat power at the defect rod can be found as

$$P = \frac{ck_0}{8\pi} \epsilon'' \int_S |E_z|^2 dS, \quad (20)$$

where c is the speed of light. The temperature difference and the absorbed power are proportional to one another,

$$\Delta\Theta = \bar{\varkappa} P, \quad (21)$$

with $\bar{\varkappa}$ being the contact heat transfer coefficient explained in the previous section. Therefore for the increment of ϵ' we have

$$\Delta\epsilon = 2\sqrt{\epsilon_0} n_1 \bar{\varkappa} \epsilon'' \frac{ck_0}{8\pi} \int_S |E_z|^2 dS. \quad (22)$$

At the resonance the dominating term in the field expansion Eq. (1) is $m = 0$ [see Fig. 1(c)]. Thus, in the defect rod we have

$$E_z(\mathbf{r}) = c_0 J_0(\sqrt{\epsilon'} k_0 r), \quad (23)$$

where c_0 is an unknown coefficient. Therefore

$$\int_S |E_z|^2 dS = |c_0|^2 \int_S J_0^2(\sqrt{\epsilon'} k_0 r) dS. \quad (24)$$

Notice that ϵ' is dependent on temperature according to Eq. (19). By matching the fields at the boundary of the defect rod one finds

$$c_0 J_0(\sqrt{\epsilon'} k_0 R_d) = a_0 J_0(k_0 R_d) + b_0 H_0^{(1)}(k_0 R_d). \quad (25)$$

Finally, after using the scattering matrix we have

$$c_0 = \frac{1}{J_0(\sqrt{\epsilon'} k_0 R_d)} \left[H_0^{(1)}(k_0 R_d) + \frac{1}{t_0(\epsilon')} J_0(k_0 R_d) \right] b_0, \quad (26)$$

where $t_0(\epsilon') = \{\hat{t}_d\}_{0,0}$ [see Eq. (9)]. By plugging Eq. (26) into Eq. (24) and then into Eq. (22), one obtains

$$\Delta\epsilon = 2\sqrt{\epsilon_0} n_1 \bar{\varkappa} \epsilon'' \frac{ck_0}{8\pi} \int_S J_0^2(\sqrt{\epsilon'} k_0 r) dS$$
$$\times \frac{1}{J_0^2(\sqrt{\epsilon'} k_0 R_d)} \left[H_0^{(1)}(k_0 R_d) + \frac{1}{t_0(\epsilon')} J_0(k_0 R_d) \right]^2 |b_0|^2. \quad (27)$$

The relationship Eq. (8) between the incident and the outgoing amplitudes can be Taylor expanded in the powers of $\Delta\epsilon$ as

$$t_0(\epsilon_0) a_0 = \left(1 - \frac{1}{t_0(\epsilon_0)} \frac{dt_0(\epsilon_0)}{d\epsilon} \Delta\epsilon \right) b_0. \quad (28)$$

Using Eq. (27) after retaining the terms up to $O(|b_0|^4)$ one obtains

$$t_0(\epsilon_0) a_0 = (1 - \Lambda |b_0|^2) b_0, \quad (29)$$

where

$$\Lambda = 2\sqrt{\epsilon_0} n_1 \bar{\varkappa} \epsilon'' \frac{ck_0}{8\pi} \frac{1}{t_0(\epsilon_0)} \frac{dt_0(\epsilon_0)}{d\epsilon} \int_S J_0^2(\sqrt{\epsilon_0} k_0 r) dS$$
$$\times \frac{1}{J_0^2(\sqrt{\epsilon_0} k_0 R_d)} \left[H_0^{(1)}(k_0 R_d) + \frac{1}{t_0(\epsilon_0)} J_0(k_0 R_d) \right]^2. \quad (30)$$

One can see that Eq. (29) accounts for the thermo-optic effect via a Kerr-like nonlinear term. Equation (29) is a complement to the linear equations (8). Together, Eqs. (8) and (30) can be
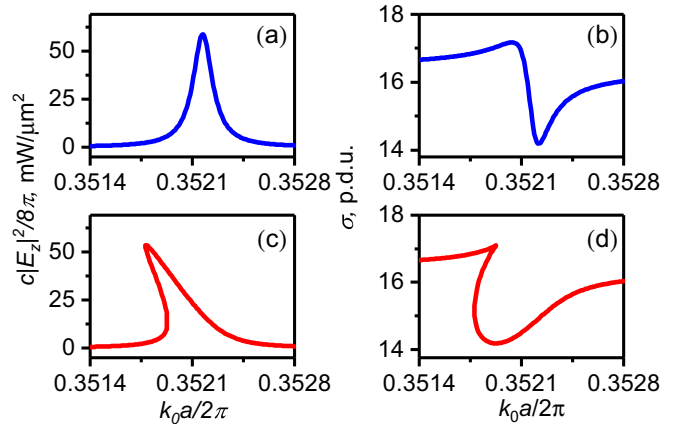
FIG. 2. Optical response from the $N \times N = 49$ array of dielectric rods. $R_0 = 0.18a$, $R_d = 0.08a$. (a), (c) The intensity of the electromagnetic field in the defect rod. (b), (d) The scattering cross section. The intensity of the incident plane wave 1.8×10^{-2} mW/μm^2 in all panels, $\epsilon'' = 10^{-3}$ in (c) and (d). The orientation of the incident **k** vector corresponds $\theta = 0$ in Fig. 1(a).
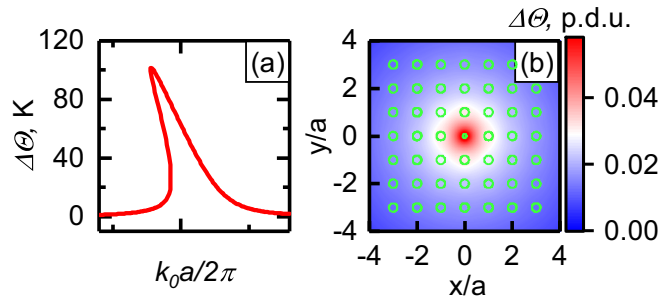
FIG. 3. Thermo-optic hysteresis in the $N \times N = 49$ array of dielectric rods. (a) Temperature of the defect rod against the incident wave number. (b) The solution of the heat equation, Eq. (14). The incident intensity 1.8×10^{-2} mW/μm^2, $\epsilon'' = 10^{-3}$. The other paremeters are the same as in Fig. 2.

substituted into Eq. (6) to produce a closed set of nonlinear equations describing light scattering in the system.

V. NUMERICAL RESULTS

Here, we apply the numerical procedure described in the previous section with $\bar{\Theta}_0$ found by solving the heat equation using the finite-element method. The picture of the optical response against the incident wave number is shown in Fig. 2. In Fig. 2 we compare the solutions with and without the account of the thermorefractive effect. The orientation of the incident **k** vector is given by angle θ [see Fig. 1(a)]. When the thermorefractiove effect is neglected we observed a typical single-resonance response in both the near field [Fig. 2(a)] and the scattering cross section [Fig. 2(b)]. When the change of the permittivity by heating is accounted for, the solution bifurcates and a nonlinear resonance is observed [see Figs. 2(d) and 2(c)]. The obtained picture of thermo-optic hysteresis can be also observed in the temperature of the defect rod. In Fig. 3(a) we demonstrate the temperature increment as a function of the incident wave number. The dependence shown in Fig. 3(a) closely follows the intensity of the electromagnetic field depicted in Fig. 2(c). Notice that the temperature increment reaches $\approx 90\,°C$ at the top of the resonance. In Fig. 3(b) we show the function $\bar{\Theta}(\bar{r})$ obtained by solving the heat equation by the finite-element method. One can see that the effect of heating is mostly observed in the unit cell containing the defect rod.

The central question to be addressed in studies on thermo-optic hysteresis is the value of the threshold intensity as dependent on the optical and geometric parameters of the system. In Fig. 4 we show the magnitude of the electric field in the defect rod that can be obtained under illumination by a plane wave at different angles of incidence and different imaginary parts of the dielectric permittivity ϵ''. The magnitudes are normalized to the maximum at a given incident intensity. The magnitude is plotted as a function of both incident intensity and detuning $\Delta \omega = \omega - \omega_0$, ω and ω_0 being the incident and resonant frequencies, correspondingly. The high magnitude spots correspond to strong resonances leading
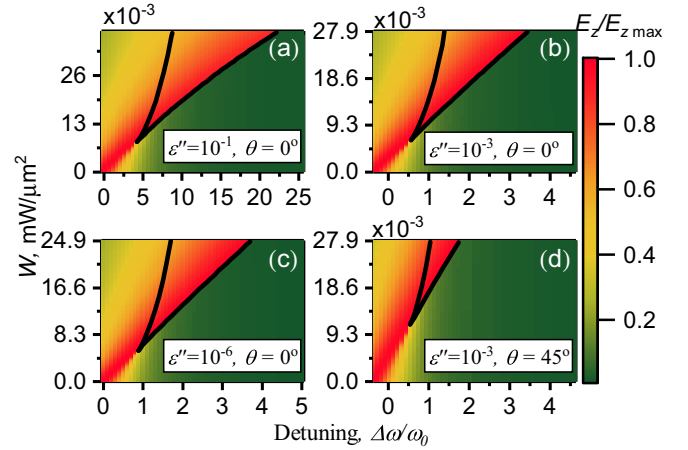
FIG. 4. The normalized magnitudes of the electric field as depended on the frequency and the intensity of the incident plane wave. The thick black lines show the boundaries of the domains with thermo-optic hysteresis. The angle of incidence and the imaginary part of the dielectric permittivity are specified in the insets. The other parameters are the same as in Fig. 2.

to heating the structure. The domains enclosed between thick black lines show the boundaries in the parameter space where the hysteresis occurs. Noticeably, the positions of the bistability domains are strongly dependent on the imaginary part of the dielectric permittivity [compare Figs. 4(b) and 4(c)]. At the same time the threshold does not depend on the orientation of the incident **k** vector although the shape of the bistability domains varies significantly [see Figs. 4(b) and 4(d)].

VI. CONCLUSION

We considered thermo-optic bistability induced by a high-quality defect mode in the square array of dielectric cylinders. It is demonstrated that the scattering problem with an account of the variation of the dielectric constant by heating can be solved with the T-matrix method by introducing an explicit dependence of the permittivity of the defect rod on temperature. The bistability can be observed both in the near field, i.e., in the amplitude of the defect mode, as well as in the far field, i.e., in the scattering cross section. We found that the bistability occurs at low intensities of the incident wave $\approx 0.01 \text{mW}/\text{μm}^2$ (see Fig. 4). This is two orders of magnitude lower than what was recently reported in Ref. [36] for a single dielectric cylinder and one order of magnitude lower than the experimental results for a silicon cantilever [35]. We believe that our results can be of used in controlling thermo-optical effects in photonic nanodevices, including engineering efficient light-to-heat conversion with the incident wavelength detuned from the wavelength of a high-quality resonance.

[1] G. P. Zograf, M. I. Petrov, D. A. Zuev, P. A. Dmitriev, V. A. Milichko, S. V. Makarov, and P. A. Belov, Nano Lett. **17**, 2945 (2017).

[2] C. Khandekar and A. W. Rodriguez, Appl. Phys. Lett. **111**, 083104 (2017).

[3] M. Aouassa, E. Mitsai, S. Syubaev, D. Pavlov, A. Zhizhchenko, I. Jadli, L. Hassayoun, G. Zograf, S. Makarov, and A. Kuchmizhak, Appl. Phys. Lett. **111**, 243103 (2017).

[4] M. Celebrano, D. Rocco, M. Gandolfi, A. Zilli, F. Rusconi, A. Tognazzi, A. Mazzanti, L. Ghirardini, E. A. A. Pogna, L. Carletti, C. Baratto, G. Marino, C. Gigli, P. Biagioni, L. Duò, G. Cerullo, G. Leo, G. D. Valle, M. Finazzi, and C. D. Angelis, Opt. Lett. **46**, 2453 (2021).

[5] J.-W. Cho, Y.-J. Lee, J.-H. Kim, R. Hu, E. Lee, and S.-K. Kim, ACS Nano **17**, 10442 (2023).

[6] F. Yang, K. Chen, Y. Zhao, S.-K. Kim, X. Luo, and R. Hu, Appl. Phys. Lett. **120**, 053902 (2022).

[7] X. Jiang and L. Yang, Light: Sci. Appl. **9**, 24 (2020).

[8] Y.-L. Tang, T.-H. Yen, K. Nishida, J. Takahara, T. Zhang, X. Li, K. Fujita, and S.-W. Chu, Opt. Mater. Express **11**, 3608 (2021).

[9] Y. Sivan and S.-W. Chu, Nanophotonics **6**, 317 (2017).

[10] C.-H. Li, Y.-L. Tang, J. Takahara, and S.-W. Chu, J. Chem. Phys. **155**, 204202 (2021).

[11] Y.-S. Duh, Y. Nagasaki, Y.-L. Tang, P.-H. Wu, H.-Y. Cheng, T.-H. Yen, H.-X. Ding, K. Nishida, I. Hotta, J.-H. Yang *et al.*, Nat. Commun. **11**, 4101 (2020).

[12] T. Zhang, Y. Che, K. Chen, J. Xu, Y. Xu, T. Wen, G. Lu, X. Liu, B. Wang, X. Xu *et al.*, Nat. Commun. **11**, 3027 (2020).

[13] Y. Kivshar, Natl. Sci. Rev. **5**, 144 (2018).

[14] D. G. Baranov, D. A. Zuev, S. I. Lepeshov, O. V. Kotov, A. E. Krasnok, A. B. Evlyukhin, and B. N. Chichkov, Optica **4**, 814 (2017).

[15] R. Masoudian Saadabad, L. Huang, and A. E. Miroshnichenko, Phys. Rev. B **104**, 235405 (2021).

[16] L. Tan, L. Yuan, and Y. Y. Lu, J. Opt. Soc. Am. B **39**, 611 (2022).

[17] D. N. Maksimov, A. S. Kostyukov, A. E. Ershov, M. S. Molokeev, E. N. Bulgakov, and V. S. Gerasimov, Phys. Rev. A **106**, 063507 (2022).

[18] M. Zhang and X. Zhang, Sci. Rep. **5**, 8266 (2015).

[19] X. Wang, J. Duan, W. Chen, C. Zhou, T. Liu, and S. Xiao, Phys. Rev. B **102**, 155432 (2020).

[20] T. Sang, S. A. Dereshgi, W. Hadibrata, I. Tanriover, and K. Aydin, Nanomaterials **11**, 484 (2021).

[21] S. Xiao, X. Wang, J. Duan, T. Liu, and T. Yu, J. Opt. Soc. Am. B **38**, 1325 (2021).

[22] Y. Cai, X. Liu, K. Zhu, H. Wu, and Y. Huang, J. Quant. Spectrosc. Radiat. Transfer **283**, 108150 (2022).

[23] G. P. Zograf, M. I. Petrov, S. V. Makarov, and Y. S. Kivshar, Adv. Opt. Photonics **13**, 643 (2021).

[24] C. W. Hsu, B. Zhen, A. D. Stone, J. D. Joannopoulos, and M. Soljačić, Nat. Rev. Mater. **1**, 16048 (2016).

[25] K. Koshelev, G. Favraud, A. Bogdanov, Y. Kivshar, and A. Fratalocchi, Nanophotonics **8**, 725 (2019).

[26] A. F. Sadreev, Rep. Prog. Phys. **84**, 055901 (2021).

[27] Z. Hu, L. Yuan, and Y. Y. Lu, Phys. Rev. A **101**, 013806 (2020).

[28] K. Koshelev, S. Lepeshov, M. Liu, A. Bogdanov, and Y. Kivshar, Phys. Rev. Lett. **121**, 193903 (2018).

[29] D. N. Maksimov, V. S. Gerasimov, S. Romano, and S. P. Polyutov, Opt. Express **28**, 38907 (2020).

[30] M. V. Rybin, K. L. Koshelev, Z. F. Sadrieva, K. B. Samusev, A. A. Bogdanov, M. F. Limonov, and Y. S. Kivshar, Phys. Rev. Lett. **119**, 243901 (2017).

[31] G. Baffou and R. Quidant, Laser Photonics Rev. **7**, 171 (2013).

[32] S. Danesi, M. Gandolfi, L. Carletti, N. Bontempi, C. De Angelis, F. Banfi, and I. Alessandri, Phys. Chem. Chem. Phys. **20**, 15307 (2018).

[33] P. Sun and R. M. Reano, Opt. Lett. **35**, 1124 (2010).

[34] G. P. Zograf, Y. F. Yu, K. V. Baryshnikova, A. I. Kuznetsov, and S. V. Makarov, JETP Lett. **107**, 699 (2018).

[35] B. Pottier and L. Bellon, SciPost Phys. **10**, 120 (2021).

[36] D. Ryabov, O. Pashina, G. Zograf, S. Makarov, and M. Petrov, Nanophotonics **11**, 3981 (2022).

[37] Y. Gao, W. Zhou, X. Sun, H. K. Tsang, and C. Shu, Opt. Lett. **42**, 1950 (2017).

[38] P. R. Villeneuve, S. Fan, and J. D. Joannopoulos, Phys. Rev. B **54**, 7837 (1996).

[39] O. Painter, J. Vučković, and A. Scherer, J. Opt. Soc. Am. B **16**, 275 (1999).

[40] G. V. Shadrina and E. N. Bulgakov, J. Exp. Theor. Phys. **135**, 632 (2022).

[41] *Electromagnetic Theory and Applications for Photonic Crystals*, edited by K. Yasumoto (CRC Press, Boca Raton, FL, 2005).

[42] https://rscf.ru/project/22-22-20056/.